

ELECTROMAGNETICALLY INDUCED TRANSPARENCY IN THE FIVE-LEVEL SCHEME OF COLD ^{85}Rb ATOMIC VAPOUR

BUI THI HONG HAI, LE VAN DOAI, DOAN HOAI SON,
DINH XUAN KHOA, AND NGUYEN HUY BANG

Vinh University, 182 Le Duan Street, Vinh City, Vietnam

PHAM VAN TRONG

Vinh University, 182 Le Duan Street, Vinh City, Vietnam

and

No 565 Quang Trung street, Dong Ve ward, Thanh Hoa City, Vietnam

LE THI MINH PHUONG

Phu Lam Technical and Economic College, Ho Chi Minh City, Vietnam

NGUYEN TUAN ANH

Ho Chi Minh City University of Food Industry, Ho Chi Minh City, Vietnam

E-mail: bangvinhuni@gmail.com

Received 09 June 2013; revised manuscript received 28 June 2013

Accepted for publication 30 June 2013

Abstract. *In the framework of the semiclassical theory, we develop an analytical approach on electromagnetically induced transparency (EIT) in the medium that consists of the five-level cascade scheme of cold ^{85}Rb atoms. In the weak field limit of the probe light, an analytical representation of EIT spectra has been derived for the first time. Signatures of EIT spectra, including transparency efficiency, have been investigated. Our theoretical results agree well with experimental observations.*

I. INTRODUCTION

Electromagnetically induced transparency (EIT) is a quantum interference effect which makes a resonance medium transparent and steep dispersive for a probe light field under induction of other strong coupling light field. The effect was introduced theoretically in 1990 [1] and experimentally verified in 1991 [2]. Since then, EIT has attracted a tremendous interest over the last years due to its unusual properties and promising potential applications, such as all optical switching [3], slow-light group velocity [4], quantum information [5], nonlinear optics at low light level [6], enhancement of Kerr nonlinearity [7], and high resolution spectroscopy [8]. Several reviews on progress in EIT effects and related applications are available [9-12] giving deeper insight into the topic and providing lists of original references.

In the early year of EIT study, three-level configurations were the main objects giving single-window EIT signature. It is worth to mention here that the linear and nonlinear

susceptibilities of such three-level systems are well understood and able to represent analytically. Such a sufficient knowledge has promoted significant progress in implementation of applications related to EIT phenomena [9].

From practical perspective, extension from single to multi-window EIT is currently of interest due to its diversifying usefulness. As an example, it is to simultaneously support slow group velocity for pulses at different frequencies [13, 14] in which the light fields have advantage in production of quantum entanglement. A possible way for obtaining multi-EIT window is to use additionally controlling fields to excite further levels (beyond three-level models). An illustration for this prototype is N -level system excited by $(N-1)$ applied electromagnetic fields giving $(N-2)$ transparent windows [15]. Another way is to use only one controlling field to couple simultaneously several closely spacing hyperfine levels. This was first demonstrated by Wang *et al* [16] for a five-level cascade scheme of cold ^{85}Rb atoms in a magneto-optical trap. Recently, Kowalski *et al* [17] numerically and experimentally reinvestigated such EIT system with some improvement in observation of EIT spectra. Although the numerical simulations were helpful to explain experimental observation [16, 17] but there still lack of analytical representation of EIT spectra. This has hampered implementation of further studies related to the five-level cascade EIT system, *e.g.*, Kerr nonlinearity, slowing-lights, and multi-wave mixing. As in several applications related to such a multi-level system, analytical representation of EIT spectra is important stage.

In this work, we develop a simple analytical method, which was applied in three-level systems [18], to EIT of the five-level cascade scheme of cold ^{85}Rb atomic medium [16, 17]. In the weak field limit of probe light, absorption and dispersion coefficients of the medium are derived in analytical forms. As an illustration for confidence of the method, we show an excellent agreement between our theoretical results and experimental observations.

II. THEORY

Let consider the five-level cascade scheme of ^{85}Rb in Fig. 1. The states $|1\rangle$, $|2\rangle$, $|3\rangle$, $|4\rangle$, and $|5\rangle$ in the left hand corresponding hyperfine components in right hand. The level separations of the $|4\rangle - |3\rangle$ and $|5\rangle - |3\rangle$ states are represent by δ_1 and δ_2 , respectively.

The states are assumed to be excited by two cw single-mode laser lights (a strong coupling and a weak probe), in which their frequency detuning from atomic resonance Δ_p and Δ_c :

$$\Delta_p = \omega_p - \omega_{21}, \quad \Delta_c = \omega_c - \omega_{32}, \quad (1)$$

where, ω_p and ω_c are frequencies of probe and coupling lasers, respectively.

In the framework of semiclassical theory, evolution of the system is represented by density operator ρ obeyed the following Liouville equation:

$$\frac{\partial \rho}{\partial t} = -\frac{i}{\hbar}[H, \rho] + \Lambda\rho, \quad (2)$$

where, H and Λ represent the total Hamiltonian and relaxation operator, respectively.

By transforming Eq. (2) into the rotating frame and using the dipole- and rotating wave- approximations, matrix elements of the system are derived as:

$$\dot{\rho}_{51} = [i(\Delta_c + \Delta_p - \delta_2) - \gamma_{51}]\rho_{51} - \frac{i}{2}\Omega_p\rho_{52} + \frac{i}{2}\Omega_c a_{52}\rho_{21}, \quad (3)$$

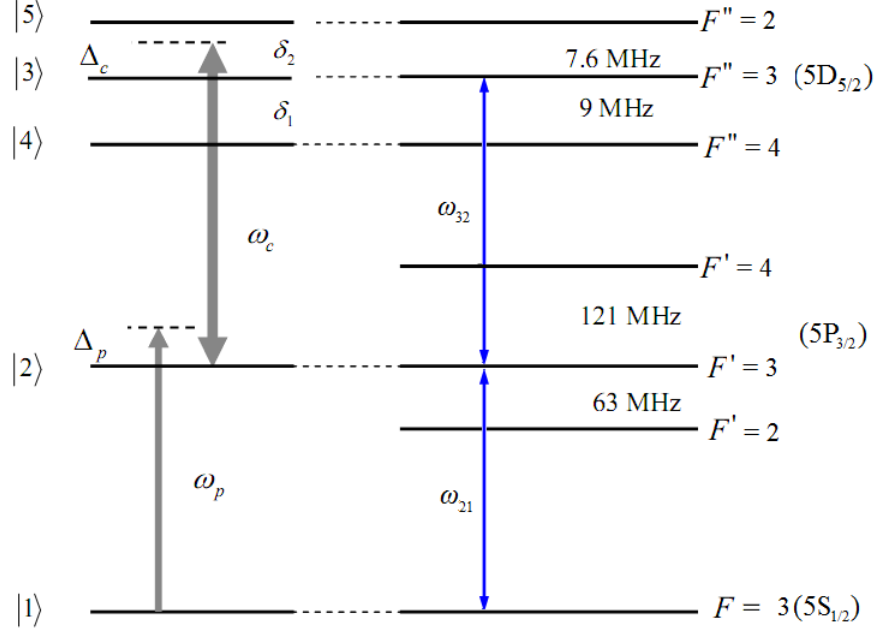


Fig. 1. The five-level cascade scheme of ^{85}Rb atom.

$$\dot{\rho}_{41} = [i(\Delta_c + \Delta_p + \delta_1) - \gamma_{41}]\rho_{41} - \frac{i}{2}\Omega_p\rho_{42} + \frac{i}{2}\Omega_c a_{42}\rho_{21}, \quad (4)$$

$$\dot{\rho}_{31} = [i(\Delta_c + \Delta_p) - \gamma_{31}]\rho_{31} - \frac{i}{2}\Omega_p\rho_{32} + \frac{i}{2}\Omega_c a_{32}\rho_{21}, \quad (5)$$

$$\dot{\rho}_{21} = [i\Delta_p - \gamma_{21}]\rho_{21} - \frac{i}{2}\Omega_p(\rho_{22} - \rho_{11}) + \frac{i}{2}a_{31}\Omega_c\rho_{31} + \frac{i}{2}\Omega_c a_{42}\rho_{41} + \frac{i}{2}\Omega_c a_{52}\rho_{51}, \quad (6)$$

where, $\Omega_p = d_{21}E_p/\hbar$ and $\Omega_c = d_{32}E_c/\hbar$ are Rabi frequencies of the probe and coupling beams, respectively; d_{ik} is transition dipole moment between the $|i\rangle$ and $|k\rangle$ states; $a_{32} = d_{32}/d_{32}$, $a_{42} = d_{42}/d_{32}$, and $a_{52} = d_{52}/d_{32}$ are the relative transition strengths of the three transitions from the three hyperfine sublevels $|3\rangle$, $|4\rangle$, and $|5\rangle$ to $|2\rangle$; γ_{ik} represents the decay rates from $|i\rangle$ to $|k\rangle$, Γ_{ik} , as follows:

$$\gamma_{ik} = \frac{1}{2} \left(\sum_{E_j < E_i} \Gamma_{ij} + \sum_{E_l < E_k} \Gamma_{kl} \right). \quad (7)$$

In the weak field limit of the probe light, most of population is in the ground state, namely,

$$\rho_{11} \approx 1, \quad \rho_{55} = \rho_{44} = \rho_{33} = \rho_{22} \approx 0. \quad (8)$$

On the otherhand, due to $\Omega_p \ll \Omega_c$ we therefore ignore the following terms: $\frac{i}{2}\Omega_p\rho_{52}$ in (3), $\frac{i}{2}\Omega_p\rho_{42}$ in (4), and $\frac{i}{2}\Omega_p\rho_{32}$ in (5). Under these assumptions, solution of the matrix

element ρ_{21} is found, in the steady regime, to be

$$\rho_{21} = \frac{-\frac{i}{2}\Omega_p}{\gamma_{21} - i\Delta_p + \frac{a_{32}^2(\Omega_c/2)^2}{\gamma_{31} - i(\Delta_p + \Delta_c)} + \frac{a_{42}^2(\Omega_c/2)^2}{\gamma_{41} - i(\Delta_p + \Delta_c + \delta_1)} + \frac{a_{52}^2(\Omega_c/2)^2}{\gamma_{51} - i(\Delta_p + \Delta_c - \delta_2)}}. \quad (9)$$

Using the matrix element ρ_{21} , the susceptibility medium for the probe light field is represented as:

$$\chi = 2 \frac{Nd_{21}}{\varepsilon_0 E_p} \rho_{21} = \frac{Nd_{21}^2}{\varepsilon_0 \hbar} \left(\frac{A}{A^2 + B^2} + i \frac{B}{A^2 + B^2} \right), \quad (10)$$

where N is density of atoms; ε_0 is the permittivity in vacuum; A and B are real parameters given by:

$$A = -\Delta_p + \frac{A_{32}}{\gamma_{31}} + \frac{A_{42}}{\gamma_{41}} + \frac{A_{52}}{\gamma_{51}}, \quad (11)$$

$$B = \gamma_{21} + \frac{A_{32}}{\Delta_p + \Delta_c} + \frac{A_{42}}{\Delta_p + \Delta_c + \delta_1} + \frac{A_{52}}{\Delta_p + \Delta_c - \delta_2}, \quad (12)$$

$$A_{32} = \frac{\gamma_{31}(\Delta_p + \Delta_c)}{\gamma_{31}^2 + (\Delta_p + \Delta_c)^2} a_{32}^2 (\Omega_c/2)^2, \quad (13)$$

$$A_{42} = \frac{\gamma_{41}(\Delta_p + \Delta_c + \delta_1)}{\gamma_{41}^2 + (\Delta_p + \Delta_c + \delta_1)^2} a_{42}^2 (\Omega_c/2)^2, \quad (14)$$

$$A_{52} = \frac{\gamma_{51}(\Delta_p + \Delta_c - \delta_2)}{\gamma_{51}^2 + (\Delta_p + \Delta_c - \delta_2)^2} a_{52}^2 (\Omega_c/2)^2. \quad (15)$$

Following the Kramer-Kronig relation, the dispersion and absorption coefficients of the medium can be determined respectively by the real and imaginary parts of the susceptibility, namely:

$$n = \frac{\omega_p n_0 \chi'}{2c} = \frac{\omega_p n_0 N d_{21}^2}{2c \varepsilon_0 \hbar} \frac{A}{A^2 + B^2}, \quad (16)$$

$$\alpha = \frac{\omega_p n_0 \chi''}{c} = \frac{\omega_p n_0 N d_{21}^2}{c \varepsilon_0 \hbar} \frac{B}{A^2 + B^2}, \quad (17)$$

where, n_0 is the background index of refraction; χ' and χ'' are the real and imaginary parts of the susceptibility, respectively.

Using (13), (14), and (15) we may define A_{k2} ($k = 3, 4, 5$) as the *effective coupling parameters* between the states $|2\rangle$ and $|k\rangle$ under induction of the solely coupling laser light. These simultaneously couplings give rise to three transparent windows. If one sets $A_{52} = A_{42} = 0$ and $A_{32} \neq 0$, the EIT spectra reduce identically to that of the three-level cascade system [17].

In order to visualize EIT spectra in a wide range of the coupling Rabi frequency, we made surface plot of α and n with the following parameters [16, 17]: $\gamma_{21} = 3$ MHz; $\gamma_{31} = \gamma_{41} = \gamma_{51} = \gamma = 0.5$ MHz; $N = 10^{14} m^{-3}$; $d_{21} = 2.5 \cdot 10^{-29} C.m$; $\Delta_c = 0$; $\delta_1 = 9$ MHz; $\delta_2 = 7.6$ MHz; and $a_{32} : a_{42} : a_{52} = 1 : 1.46 : 0.6$. Surface plots of absorption and dispersion coefficients are represented in Fig. 2.

Although the coupling laser frequency is on resonance with the $5P_{3/2}(F' = 3) - 5D_{5/2}(F'' = 3)$ transition but a three-window EIT is appeared. This behavior is due to the strong coupling field induces simultaneously the three levels $5D_{5/2}(F'' = 4, 3, 2)$.

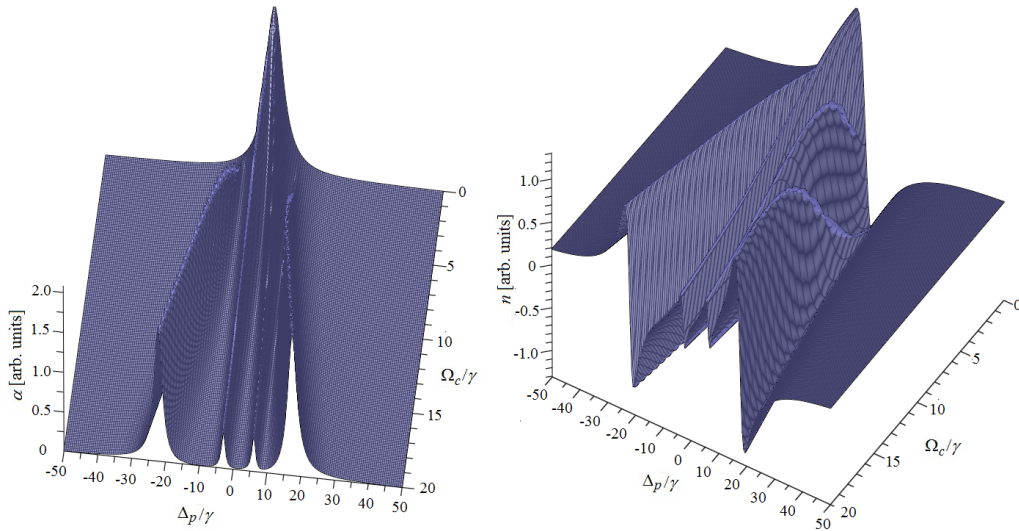


Fig. 2. Surface plots of absorption (*left*) and dispersion (*right*) with respect to probe frequency detuning Δ_p and coupling Rabi frequency Ω_c when $\Delta_c = 0$.

In order to see the influence of frequency detuning of the coupling field, we plot the absorption and dispersion coefficients with $\Omega_c = 15$ MHz, as in Fig. 3. It is easy to see EIT window position (also dispersion) is shifted with respect to frequency detuning of the coupling field.

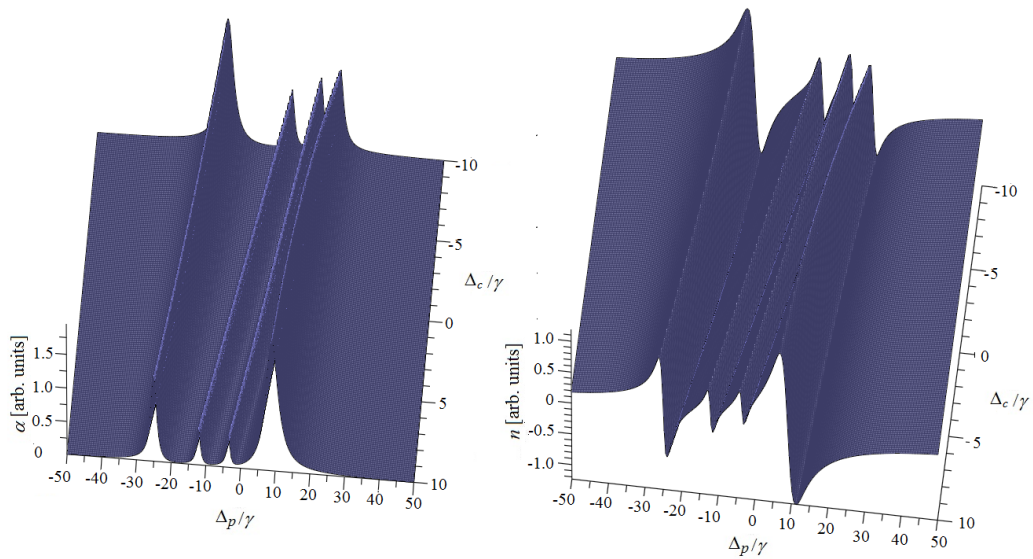


Fig. 3. Surface plots of absorption (*left*) and dispersion (*right*) with respect to frequency detuning of the probe and coupling fields, respectively.

In order to see the influence of coupling intensity on the transparent efficiency, we defined transparency efficiency by:

$$R_{EIT} = \frac{\alpha_{off} - \alpha_{on}}{\alpha_{off}} \times 100\% = \left(1 - \frac{B}{A^2 + B^2} \frac{\gamma_{21}^2 + \Delta_p^2}{\gamma_{21}} \right) \times 100\% \quad (18)$$

where, α_{on} and α_{off} denote the absorption coefficients (given by expression (17)) for the presence and absence of the coupling light beam, respectively. The dependence of R_{EIT} on coupling intensity for the three windows is shown in Fig. 4.

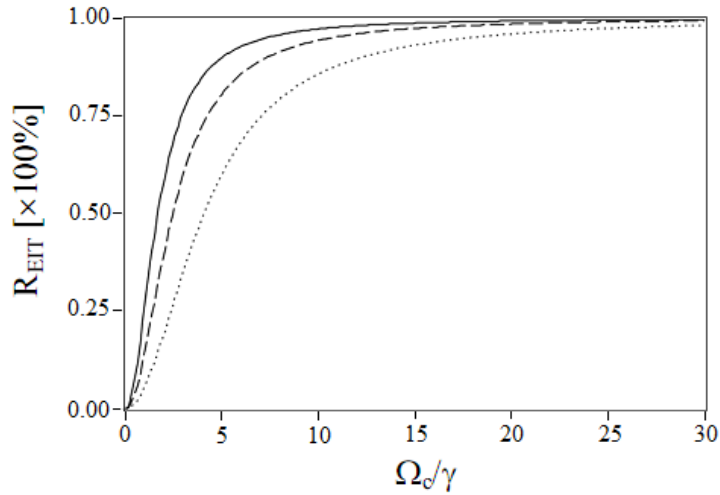


Fig. 4. Dependence of R_{EIT} on coupling intensity for the three windows corresponding to transitions: $|2\rangle \leftrightarrow |4\rangle$ (solid-line), $|2\rangle \leftrightarrow |3\rangle$ (dashed-line), and $|2\rangle \leftrightarrow |5\rangle$ (dotted-line).

From Fig. 4, we may see a highest and lowest efficiency for the case of $|2\rangle \leftrightarrow |4\rangle$ and $|2\rangle \leftrightarrow |5\rangle$ transition, respectively. This signature can be explained by coupling strength ratio $a_{42}:a_{32}:a_{52} = 1.46:1:0.6$, thus results in the effective coupling parameters $A_{42} > A_{32} > A_{52}$ at their centers (see (13), (14), and (15)).

III. COMPARISON WITH EXPERIMENTAL OBSERVATION

In order to test the confidence of the analytical results, we compared the theoretical results with the experimental transmission EIT spectra observed in [17]. Since laser linewidths (γ_c for the coupling and γ_p for the probe) used in the experiment were about 1 MHz, we therefore have to account its influence on the analytical EIT spectra. By assuming Lorentzian profile of the laser spectral lines, their linewidths are thus incorporated into atomic decaying rates [18] for this purpose, namely: $\gamma_{21} \rightarrow \gamma_{21} + \gamma_p + \gamma_D \approx 4.5$ MHz, $\gamma_{31} = \gamma_{41} = \gamma_{51} \rightarrow \gamma_{31} + \gamma_c + \gamma_p + \gamma_D \approx 2.5$ MHz; here, $\gamma_D \approx 0.2$ MHz is Doppler linewidth of cold atoms in the experimental condition. The comparison is given in Fig. 5, where it shows a tremendous agreement between the theoretical and experimental EIT spectra.

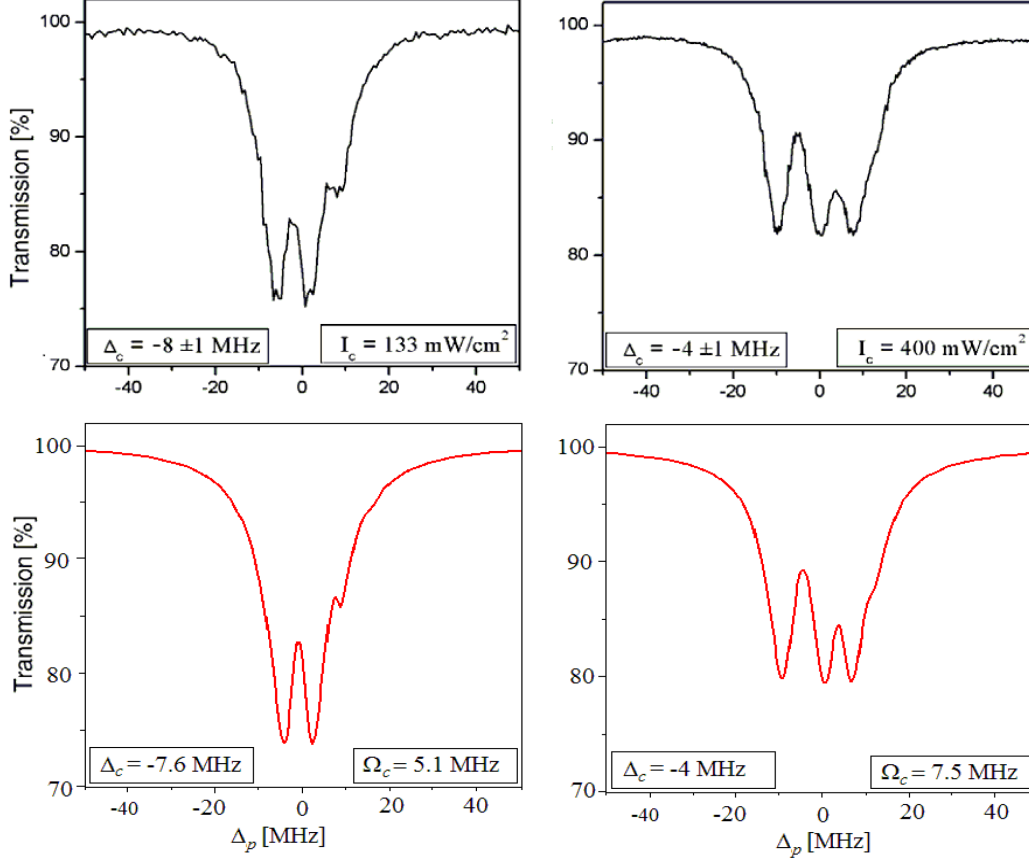


Fig. 5. Transmission EIT spectrum observed experimentally in Ref. 17 (*upper*), and our theoretical results (*lower*) at different values of frequency detuning and coupling intensity (Rabi frequency).

IV. CONCLUSIONS

In the weak field limit for probe light, analytical representation of EIT spectra of the five-level cascade system of ^{85}Rb cold atoms has been derived for the first time. The multi-EIT window signatures are investigated theoretically, and compared to experimental observation showing a good agreement. We believe that the analytical form derived in this work is comfortable for investigation of EIT signatures and useful for further studies related to multi-window EIT media, such as slow-light, EIT enhanced Kerr nonlinearity, and multi-wave mixing.

ACKNOWLEDGMENT

The financial support from the Vietnam's National Foundation for Science and Technology Development (NAFOSTED) under the project code 103.06.110.09 is acknowledged.

REFERENCES

- [1] S. E. Harris, J.E. Field, and A. Imamoglu, *Phys. Rev. Lett.* **64** (1990) 1107.
- [2] K. J. Boller, A. Imamoglu, and S.E. Harris, *Phys. Rev. Lett.* **66** (1991) 2593.
- [3] B. S.Ham, *J. Mod. Opt.* **49** (2002) 2477.
- [4] L. V. Hau, S. E. Harris, Z. Dutton, and C.H. Bejroozi, *Nature* **397** (1999) 594.
- [5] M. D. Eisaman, A. Andre, F. Massou, M. Fleischhauer, A. S. Zibrov, and M. D. Lukin, *Nature* **438** (2005) 837.
- [6] S. E. Harris and Lene Vestergaard Hau, *Phys. Rev. Lett.* **82** (1999) 4611.
- [7] H. Wang, D. Goorskey, and M. Xiao, *Phys. Rev. Lett.* **87** (2001) 073601.
- [8] A. Krishna, K. Pandey, A. Wasan, and V. Natarajan, *Eur. Phys. Lett.* **72**(2) (2005) 221.
- [9] A. Joshi and Min Xiao, *Progress in Optics* **49** (2006) 97.
- [10] J. P. Marangos, *J. Mod. Opt.* **45** (1998) 471.
- [11] M. D. Lukin, *Rev. Mod. Phys.* **75** (2003) 457.
- [12] M Fleischhauer, A Imamoglu, and J P Marangos, *Rev. Mod. Phys.* **77** (2005) 633.
- [13] M. D. Lukin, A. Imamoglu, *Phys. Rev. Lett.* **84** (2000) 1419
- [14] Y. Li, C. Hang, L. Ma, G. Huang, *Physics Letters A* **354** (2006) 1-7.
- [15] D. McGloin, D.J. Fullton, and M.H.Dunn, *Opt. Commu.* **190** (2001) 221.
- [16] J. Wang, L. B. Kong, X. H. Tu, K. J. Jiang, K. Li, H. W. Xiong, Yifu Zhu, and M. S. Zhan, *Phys. Lett.* **A328** (2004) 437-443.
- [17] K. Kowalski, V. Cao Long, H. Nguyen Viet, S. Gateva, M. Głódz, J. Szonert, *Journal of Non-Crystalline Solids* **355** (2009) 1295-1301
- [18] Julio Gea-Banacloche, Yong-qing Li, Shao-zheng Jin, and Min Xiao, *Phys. Rev.* **A51** (1995) 576.